HHS Public Access

Author manuscript

J Cancer Sci Ther. Author manuscript; available in PMC 2017 January 30.

Published in final edited form as:

J Cancer Sci Ther. 2016 ; 8(7): 172–178. doi:10.4172/1948-5956.1000410.

Anti-VEGFR2 driven nuclear translocation of VEGFR2 and acquired malignant hallmarks are mutation dependent in glioblastoma

Adarsh Shankar, B.S., **Meenu Jain, Ph.D.**, **Mei Jing Lim**, **Kartik Angara**, **Peng Zeng, M.D.**, **Syed A. Arbab**, **ASM Iskander, M.D.**, **Roxan Ara, M.D.**, **Ali S. Arbab, M.D., Ph.D.**, and **Bhagelu R. Achyut, Ph.D.**[*]

Tumor Angiogenesis Lab, Cancer Center, Augusta University, 1410 Laney Walker Blvd, CN3124A, Augusta, GA 30912, USA

Abstract

Objective—Anti-angiogenic therapies (AATs), targeting VEGF-VEGFR pathways, are being used as an adjuvant to normalize glioblastoma (GBM) vasculature. Unexpectedly, clinical trials have witnessed transient therapeutic effect followed by aggressive tumor recurrence. In pre-clinical studies, targeting VEGFR2 with vatalanib, increased GBM growth under hypoxic microenvironment. There is limited understanding of these unanticipated results. Here, we investigated tumor cell associated phenotypes in response to VEGFR2 blockade.

Methods—Human U251 cells were orthotopically implanted in mice (day 0) and were treated with vehicle or vatalanib on day 8. Tumor specimens were collected for immunohistochemistry and protein array. Nuclear translocation of VEGFR2 was analyzed through IHC and western blot. *In vitro* studies were performed in U251 (p53 and EGFR mutated) and U87 (p53 and EGFR wildtype) cells following vehicle or vatalanib treatments under normoxia (21% O_2) and hypoxia (1% O_2). Proliferation, cell cycle and apoptosis assays were done to analyze tumor cell phenotypes after treatments.

Results—Vatalanib treated animals displayed distinct patterns of VEGFR2 translocation into nuclear compartment of U251 tumor cells. *In vitro* studies suggest that vatalanib significantly induced nuclear translocation of VEGFR2, characterized in chromatin bound fraction, especially in U251 tumor cells grown under normoxia and hypoxia. Anti-VEGFR2 driven nuclear translocation of VEGFR2 was associated with increased cell cycle and proliferation, decreased apoptosis, and displayed increased invasiveness in U251 compared to U87 cells.

Conclusions—Study suggests that AAT- induced molecular and phenotypic alterations in tumor cells are associated with mutation status and are responsible for aggressive tumor growth. Therefore, mutation status of the tumor in GBM patients should be taken in to consideration before applying targeted therapy to overcome unwanted effects.

[*]CORRESPONDING AUTHOR: Bhagelu R. Achyut, PhD, Assistant Research Scientist, Tumor Angiogenesis Lab, Cancer Center, Augusta University, 1410 Laney Walker Blvd, CN3124A, Augusta, GA 30912, USA, Tel: 706-721-9344, Fax: 706-434-6406, bachyut@augusta.edu.

CONFLICT OF INTEREST: None

Keywords

Glioblastoma; anti-angiogenic therapy; resistance; VEGFR2; nuclear translocation; mutation; tumor cells; hypoxia

INTRODUCTION

Glioblastoma (GBM) is considered as hypervascular, hypoxic and most malignant form of glioma [1, 2]. GBM is most lethal during first year after initial diagnosis despite surgical resection, radiotherapy and/or chemotherapy [2]. Anti-angiogenic therapies (AAT) are being used as an adjuvant mainly against vascular endothelial growth factor and its receptors (VEGF-VEGFRs) in endothelial cells to normalize tumor vasculatures [3, 4]. Due to lower genetic instability in endothelial cells compared to in tumor cells, it was anticipated that targeting VEGF-VEGFR pathways, primarily in endothelial cells, would decrease tumor vasculature without imposing drug resistance. However, treatments provided minimal to none effect with no change in overall patients survival [3, 4].

Similar data was obtained from preclinical studies. For example, VEGFR2 blockade in GBM through vatalanib, a receptor tyrosine kinase inhibitor, increased tumor size [5] through hypoxia mediated overexpression of VEGF, SDF-1α, HIF-1α, VEGFR2, VEGFR3 and EGFR at peripheral part of tumors compared to central part [6]. Activation of alternative pathways of angiogenesis, vasculogenesis and involvement of stem cells were observed following AAT in GBM [7], which was associated with overexpression of bFGF, angiopoietin1/2, GCSF, and SDF1α [5]. Conventionally, tumor vessel formation occurs through angiogenesis, which is mediated by proliferation and migration of resident ECs[8]. However, at a cellular level, up-regulation of HIF-1α and SDF-1α by tumor cells [9] resulted into recruitment of CXCR4+ bone marrow derived cells (BMDCs) to the tumor [10]. BMDCs play a pivotal role in tumor development. Endothelial progenitor cells (EPCs) from BM pool are recruited in tumor microenvironment (TME) and contributed to vasculogenesis [10, 11]. Recently, we discovered that VEGFR2 blockade increased myeloid and angiogenic cell signatures that contributed to the increased vasculature [12]. CSF1R blockade identified host derived and ERK regulated CXCL7 as a mediator of myeloid cell response and antiangiogenic resistance [12]. Moreover, previous studies have reported the effects of VEGF-VEGFR blockade on development of endothelial cell-associated tumor vasculature and BMDCs mediated vasculogenic mechanisms [13, 14]. In addition to stroma associated mechanisms, tumor cell mediated mechanisms may contribute to AAT resistance.

Interestingly, we noticed that VEGF receptors are highly expressed in tumor cells and effect of VEGFR2 blockade on GBM tumor cells is largely unexplored. Therapeutic responses and treatment efficacies of AATs has been known to be affected by mutational burden and epigenetic alterations in tumor [2, 15, 16]. However, effect of VEGFR2 blockade on GBM associated mutational heterogeneity in tumor cells is poorly understood. Here, we investigated fate of VEGFR2 expression in human tumor cell lines (p53 and EGFR mutated versus wild-type) following anti-VEGFR2 treatment in GBM models. Anti-VEGFR2 induced nuclear translocation and chromatin bound VEGFR2 in GBM cell lines were

associated with increased invasion, migration, cell cycle, and proliferation in p53 and EGFR mutated tumor cell lines compared to p53 and EGFR normal. Study supports that mutation status of the tumor in GBM patients should be taken in to consideration before applying targeted therapy to overcome unwanted effects.

METHODS

Ethics statement

Animal protocol (#2014-0625) was approved by Institutional Animal Care and Use Committee (IACUC) and Institutional Review Board of Augusta University. All efforts were made to ameliorate suffering of animals. CO_2 with secondary method was used to euthanize animals at the end of study.

Chimeric mouse and human GBM model

Human GBM in chimeric mouse was established and animals were treated with vatalanib as reported previously [12, 17].

Cell culture study

Human GBM cell lines, U251 and U87 (differ in p53 and EGFR mutations)[18], were cultured in high glucose DMEM supplemented with 10% FBS, 4.0 Mm L-Glutamine and 4500 mg/L Glucose (Thermo Scientific). Recombinant human VEGF (4ng/ml, Prospecbio, Israel) was added to culture media and treated with vehicle or vatalanib (10 μM). Culture flasks (normoxia (21% O_2), normoxia+ vatalanib, hypoxia (1% O_2) and hypoxia+ vatalanib) were incubated at 37°C and 5% CO_2 for 48 hours.

Immunohistochemical staining

Standard procedures were performed on tissues as well as smears of cultured tumor cells on glass slides, as recommended by VEGFR2 antibody supplier (Abcam, USA). Following IHC, nuclear staining of VEGFR2 was quantified blindly by two different investigators. Invasive tumor cells were analyzed using CD44 (Abcam) staining under a fluorescence microscope (Carl Zeiss).

Protein Array

Vehicle and vatalanib treated tumor protein, and *in vitro* cultured U251 tumor cell supernatant were collected for customized human cytokine array (Ray Biotech).

Western Blot Analysis

Cells were collected and processed for protein isolation using T-PER, (tissue protein extraction reagent) for tissue and Pierce RIPA buffer for tumor cells (Thermo Scientific, USA). Total protein was separated by Tris/Glysine/SDS gel electrophoresis. Membranes were incubated with primary antibodies against HIF1α (1:1000, R&D), VEGFR2 (1:1000, Abcam), phospho-P38, total-P38, phospho-ERK, total-ERK phospho-AKT and total-AKT (1:1000, Cell signaling), ID1 (1:1000, Biocheck, USA), β-actin (1:5000, Sigma), and HRP-conjugated secondary antibody (1:5000, Biorad).

For nuclear translocation studies, tumor cells were collected after 48 hours of cell culture and proteins from sub-cellular compartments were prepared using protein fractionation kit (Thermo Scientific, USA). VEGFR2 (Abcam) were detected in all compartments. Each of the compartments had different loading controls (Abcam): cell membrane (HSP-60), Nuclear (Lamin A/C), chromatin (Histone H3), cytoplasmic and cytoskeletal (β-actin, Sigma). Western blot images were acquired by Las-3000 imaging machine (Fuji Film, Japan).

Cell viability by MTT (3-(4,5-Dimethylthiazol-2-yl)-2,5-diphenyltetrazoliumbromide) assay

Individual well of a 96-well plate was inoculated with 100 μl of medium containing 5×10^4 cells. Cells were incubated in medium with 10μM concentration of vatalanib prepared in DMSO for 24 and 48 hours. MTT assay was performed as recommended by manufacturer (Roche, USA) Absorbance for MTT was measured at 570 nm by the ELISA Plate reader VICTOR3 (PerkinElmer, USA). Cell viability (%) for all groups was normalized to normoxia 24 hours sample. All experimental samples were run in triplicates and performed twice.

Reactive Oxygen Species (ROS) assay

U251 and U87 cell lines were cultured in regular culture conditions. VEGF was added, along with 10μM final concertation of ROS agent (Molecular Probes), and kept in 37°C for 30 minutes, allowing ROS agent to probe into the cell. After washing plates with 1X PBS cells were treated with vatalanib (10μM). Plates were allowed for 4-hour incubation at 37°C and fluorescent activity was acquired via fluorescence VICTOR3 (PerkinElmer, USA).

Apoptosis Assay

Vehicle and vatalanib treated U251 and U87 GBM tumor cells were harvested after 48 hours of culture under hypoxic and normoxic conditions. Cell apoptosis analysis was performed using CY3-annexin V and 7AAD cell labeling using apoptosis detection kit (BD Pharmingen, USA). Cells were harvested and labeled with CY3-Annexin V and 7AAD for 15 minutes in a dark place. Cell apoptosis distribution was analyzed using Accuri C6 machine (BD Biosciences).

Cell cycle assay

Vehicle and vatalanib treated U251 and U87 GBM tumor cells were harvested after 48 hours of culture under hypoxic and normoxic conditions. Cells were harvested and fixed in 70% ethanol at 4°C overnight. Cells were stained with propidium iodide (PI) (Biolegend, USA) solution at a final concentration of 50 μg/ml containing 50 μg/ml RNase A. Cell cycle data was acquired and analyzed using Accuri C6 machine.

Statistical analysis

Quantitative data was expressed as mean ± SD and analyzed through Student t-test using GraphPad Prism. Differences were considered statistically significant at p value <0.05.

RESULTS

Vatalanib treatment induced nuclear translocation of VEGFR2 in human GBM model

U251 tumor cells were orthotopically implanted in chimeric mice on day 0 and vatalanib treated from day 8 (established tumors) [12, 19, 5]. Vehicle and vatalanib treated tumor tissues were collected on endpoint (day 22) and processed for VEGFR2 IHC (Figure 1A). Vehicle treated tumors displayed mostly membrane bound VEGFR2 (yellow arrows). However, vatalanib treated tumors displayed significantly increased nuclear VEGFR2 (red arrows) compared to vehicle (Figure 1A&B).

As expected, HIF1α was increased under hypoxia compared to normoxia in both tumor cell lines. Surprisingly, HIF1α expression was decreased after vatalanib treatment in U251 and increased after vatalanib treatment in U87 under hypoxia. This could be associated with p53 mediated regulation of HIF1α[20]. Following vatalanib treatment, total VEGFR2 expression was increased under normoxia compared to vehicle in both cell lines. Hypoxia increased VEGFR2 expression compared to normoxia. (Figure 1C).

VEGFR2 expression in cellular compartments of tumor cell lines was analyzed. In U251 cells, VEGFR2 expression was lower in membrane compartment both in vatalanib and vehicle treated samples, under hypoxia compared to normoxia. The cytoplasmic compartment showed similar patterns as membrane compartment, in which hypoxia had lower expression, when compared to normoxia. Increased VEGFR2 was seen in cytoskeletal compartment in normoxia with vatalanib, when compared to normoxia and vehicle. No change in soluble nuclear compartment was seen. In chromatin bound compartment, vatalanib groups had a clear increase in expression, when compared to vehicle, both in normoxia and hypoxia (Figure 1C). The U87 cell lines had similar observations to that of U251 cells for the membrane compartment, except a significant decrease in vatalanib group in normoxia. We observed lower expression in cytoplasm compartment in both conditions, but no changes between treatments. The cytoskeletal compartment showed no changes, while there was an increase in vatalanib group under normoxia, in soluble nuclear compartment. We also observed an increase in expression in vatalanib group under normoxia in chromatin bound compartment (Figure 1C).

Immunocytochemical analysis of cultured U251 and U87 tumor cell smears showed increased nuclear expression of VEGFR2 in vatalanib treated normoxic cells compared to vehicle, except vatalanib treatment decreased nuclear VEGFR2 under hypoxia in U87 cells (Figure 1D).

Vatalanib treatment and cell viability

MTT assay was performed at 24 and 48 hours to evaluate the cell viability following vatalanib treatment at 10μM dose. Increased number of viable U251 cells were observed in 48 hours of vatalanib treatment under normoxia as well as hypoxia compared to 24 hours of vehicles. (Supplementary Fig. S1).

Vatalanib treatment induced cell cycle and proliferation

In U251 cells, vatalanib treatment did not alter G0/G1, S and G2/M phases under normoxia compared to vehicle treated group (56.4%, 23% and 14.5% versus 52.8%, 21.4% and 15.3%, respectively). However, vatalanib significantly increased G2/M phase under hypoxia condition compared to vehicle treated group (GO/G1, S and G2/M: 47.6%, 32.6% and 5.1% versus 49.3%, 29.3% and 14.1%, respectively) (Figure 2A). In U87 cells, vatalanib treatment resulted into G0/G1 arrest under normoxia compared to vehicle treated group (GO/G1, S and G2/M: 50.6%, 22% and 20.1% versus 61.2%, 15.6% and 12.3%, respectively). However, vatalanib treatment did not alter G0/G1, S and G2/M phases under hypoxia condition compared to vehicle treated group (GO/G1, S and G2/M: 55.3%, 26.2% and 7.4% versus 53.9%, 24.1% and 9.2%, respectively). This clearly indicated that vatalanib increased the proliferation under hypoxia when compared to vehicle group (Figure 2A). Vatalanib treatment increased phospho-ERK expression, which indicated active proliferation [21], both in normoxia and hypoxia conditions in U251 cells. There was no change in phospho-ERK expression in U87 groups (Figure 2B).

Vatalanib treatment decreased apoptosis

Cells were grouped into viable, apoptotic and dead populations based on annexin V and 7AAD staining patterns on plot. Increased viable U251 cells and decreased dead cells were seen with vatalanib compared to vehicle treatment under normoxia with no change in apoptosis (viable: 18.2% versus 21.8%, dead: 12.2% versus 8.2%, apoptotic: 69.5% versus 69.8%, respectively). Surprisingly, significant increased viable cells and decreased apoptotic cells were seen with vatalanib treatment under hypoxia condition (viable: 37.9% versus 51.3%, apoptotic: 58.6% versus 46%, respectively) (Figure 3A).

In U87 cells, vatalanib compared to vehicle treatment under normoxia increased live cells (15.4% versus 19.8%) and decreased apoptotic cells (77.8% versus 66.6%). Similar trends were seen in vehicle versus vatalanib under hypoxia condition (viable: 37.5% versus 49.1%, dead: 5.7% versus 7%, apoptotic: 56.7% versus 43.4%, respectively) (Figure 3A). Further, we noticed decreased cleaved PAPR expression, which indicated reduced apoptosis, both in U251 and U87 cells under hypoxia compared to normoxia groups (Figure 3B).

Vatalanib treatment induced invasion and migration

Vatalanib induced chemokines and their receptors (EGF-EGFR, TGFβ1-TGFβR2, PDGFAA- PDGFRA, MMP2 and MMP9) in culture supernatant, especially under hypoxia (Figure 4A). These factors are known to be involved in invasion and migration of tumor cells. We investigated if ROS production has influence on cellular motility (39). In U251 cells, hypoxia showed higher ROS production than normoxia in vehicle group. In U87 cells, vatalanib compared to vehicle treatment decreased ROS production both in normoxia and hypoxia (Supplementary Fig. S2). This could be partially associated with the decreased U87 cell motility. U251 cells were pre-treated with vatalanib for 48 hours and grown under normoxia for 12 hour, which showed increased cell migration compared to vehicle, as shown by scratch assay (Supplementary Fig. S3A). No difference in migration was seen in U87 cells, when grown and treated similarly (Supplementary Fig. S3B).

Vatalanib increased phospho-P38 and ID1 protein expression, indicating active invasion in U251 cells under both normoxia and hypoxia compared to vehicle (Figure 4B). In U87 cells, vatalanib decreased phospho-P38 expression under normoxia compared to vehicle. Vatalanib did not modulate P38 under hypoxia condition and resulted into complete loss of phospho-P38. ID1, an inhibitor of basic helix-loop-helix transcription factors, has recently been shown to be a key regulator of invasiveness and metastatic potential of cancers [22]. 1D1 expression was increased after vatalanib treatment under normoxia compared to vehicle. Hypoxia decreased ID1 expression, which did not modulate by vatalanib (Figure 4B). However, U87 showed upregulation only in normoxia. Hypoxia significantly decreased 1D1 expression in U87 cells.

Phospho-AKT has been reported to promote glioma cell survival [21]. Overall, p-AKT was upregulated in hypoxia compared to normoxia in both U251 and U87. Interestingly, vatalanib decreased p-AKT compared to vehicle under normoxia in U251 cells. No difference was seen under hypoxia. However, vatalanib increased p-AKT compared to vehicle under hypoxia in U87 cells (Figure 4B).

In addition, vatalanib treated tumor acquired mesenchymal features (CD44+) (Figure 4D). CD44+ tumor periphery was accompanied with band of GFP+ stroma in vatalanib treated tumors (Figure 4C). Recently, study reported that tumor aggressiveness is associated with CD44/c-Met signaling cascade[23]. Our study suggested that CD44 expression is associated with invasiveness following vatalanib treatment in U251 tumors.

DISCUSSION

Since GBM is hypervascular in nature, vatalanib, Sunitinib, etc. have been tested against VEGF-VEGFR pathway to control abnormal vasculature in clinical trials [7]. Unexpectedly, treatments were transitory and showed incomplete efficacy with enhanced tumor burden, causing therapeutic resistance [24]. Neovascularization is one of the hallmarks of drug resistance, when VEGF-VEGFR pathway was targeted in GBM [12, 19, 5, 3, 4]. In the present study, vatalanib was selected due to its demand in several past and ongoing clinical trials (https://clinicaltrials.gov). So far, studies reported the effect of VEGFR2 blockade on endothelial cell related vasculature in tumors. Current study is an attempt to show how AAT induced therapeutic resistance by enhancing cancer hallmarks using GBM as a model tumor and vatalanib as a model drug. Therapeutic responses are variable among GBM patients and animal tumor models due to genetic heterogeneity and differential mutational load, therefore, study was done with two GBM cell lines, which differ in mutation status.

We noticed that VEGFR2 was highly expressed in tumor cells, and we investigated the fate of VEGFR2 in tumor cells following vatalanib treatment in animal model and *in vitro* studies. Study provided evidence of AAT induced molecular and phenotypic reprograming of tumor cells into malignant cells, partly due to nuclear translocation of membranous VEGFR2 and chromatin regulation. Data indicated that vatalanib induced nuclear translocation of VEGFR2 may have critical role in invasion and proliferation hallmarks. Previously, study reported that VEGFR2, a major mediator of angiogenic effects of VEGF, was translocated to the endothelial cell nucleus in response to VEGF. VEGFR2 interacted

with SP1 transcription factor at its own promoter (−300/−116, relative to transcription start site) to drive VEGFR2 transcription [25, 26]. This was further confirmed by blocking VEGF-VEGFR pathway using Bevacizumab and Sunitinib in endothelial cells, which blocked nuclear translocation of VEGFR2 [25]. Nuclear translocation of VEGFR2 was associated with cell cycle, endothelial cell growth and proliferation, cell movement etc.[25]. We anticipate that vatalanib induced VEGFR2 nuclear translocation in GBM tumor cells may have similar regulatory functions. However, we did not study in-depth regulatory mechanisms in this report.

We noticed vatalanib, which has broad range of tyrosine kinase inhibition, induced cell cycle and proliferation, decreased apoptosis and increased invasion and migration in U251 cells. However, these cancer hallmarks were induced differently by vatalanib and hypoxia in U87 cells, in part, due to genetic differences associated with these cell lines, especially p53 and EGFR mutations [18]. This data is supported by several failed clinical trials and preclinical studies involving AATs, where treatment initially showed decreased tumor volume but later displayed aggressive relapse. These reports suggest that GBM or grade IV astrocytoma is difficult to treat probably due to presence of mutational loads. On the other hand, some preclinical studies have reported the beneficial effect of several AATs. They selected human U87 cell line that does not reflect true features of GBM and have less mutational load[18].

For example, SU1498, which is a different class of VEGFR2 inhibitor, abrogated VEGFR2 activity and inhibited vascular functions and signaling cascade in U87 and patient derived cells through suppressing FAK and MAPK ERK1/2 pathways [27]. In contrast, blockade of VEGF activity by Bevacizumab failed to recapitulate the impact of SU1498, suggesting that VEGFR2 -mediated neovascularization is independent of VEGF in U87 cells [27]. Similarly SU1498 treatment promoted apoptosis in U87 cells in culture [28]. VEGFR2 inhibition using monoclonal antibody (DC101) either alone or in combination with VEGFR1 monoclonal antibody/photodynamic therapy significantly reduced the tumor volume through increased tumor cell apoptosis and prolonged the survival time of U87 implanted animals [29]. The present study and previous data suggests that U87 model displays key dissimilarities to the U251 model and human GBM at the histopathological level [30]. In contrast with human GBM, tumor vasculature in U87 model displayed significantly homogeneous vessels, which favored better access of systemic drugs to the tumor sites, as discussed in above studies involving U87 cell line models [31]. Previously, we have modeled human GBM in preclinical studies with U251 tumors and found similar histological and therapeutic features as shown by failed clinical trials [12, 19]. However, preclinical use of patient derived xenograft for therapeutic studies will provide clear picture of variations associated with the therapeutic responses among individuals[32].

In summary, vatalanib treated animals displayed distinct patterns of VEGFR2 translocation into nuclear compartment of tumor cells, which was associated with increased cell cycle and proliferation, decreased apoptosis, and displayed increased invasiveness or migration capabilities. Interestingly, U251 and U87 tumor cells showed variation in VEGFR2 nuclear translocation, cell cycle, proliferation, apoptosis, invasion, and migration probably due to differences in mutational status. Altogether, studies suggest that AAT-induced molecular and phenotypic alterations in tumor cells are associated with the mutational load and are

responsible for therapeutic failures in GBM. Therefore, patients are required to group on the basis of mutation load to limit the AAT associated therapeutic resistance in GBM.

Supplementary Material

Refer to Web version on PubMed Central for supplementary material.

Acknowledgments

FINANCIAL SUPPORT: National Institutes of Health grants R01CA160216 and R01CA172048 to Dr. Arbab.

References

1. Brat DJ, Van Meir EG. Vaso-occlusive and prothrombotic mechanisms associated with tumor hypoxia, necrosis, and accelerated growth in glioblastoma. Laboratory investigation; a journal of technical methods and pathology. 2004; 84:397–405. [PubMed: 14990981]
2. Olar A, Aldape KD. Using the molecular classification of glioblastoma to inform personalized treatment. The Journal of pathology. 2014; 232:165–177. [PubMed: 24114756]
3. Jain RK. Antiangiogenesis Strategies Revisited: From Starving Tumors to Alleviating Hypoxia. Cancer cell. 2014; 26:605–622. [PubMed: 25517747]
4. Jayson GC, Kerbel R, Ellis LM, Harris AL. Antiangiogenic therapy in oncology: current status and future directions. Lancet. 2016
5. Ali MM, Kumar S, Shankar A, Varma NR, Iskander AS, et al. Effects of tyrosine kinase inhibitors and CXCR4 antagonist on tumor growth and angiogenesis in rat glioma model: MRI and protein analysis study. Translational oncology. 2013; 6:660–669. [PubMed: 24466368]
6. Ali MM, Janic B, Babajani-Feremi A, Varma NR, Iskander AS, et al. Changes in vascular permeability and expression of different angiogenic factors following anti-angiogenic treatment in rat glioma. PloS one. 2010; 5:e8727. [PubMed: 20090952]
7. Dietrich J, Norden AD, Wen PY. Emerging antiangiogenic treatments for gliomas - efficacy and safety issues. Curr Opin Neurol. 2008; 21:736–744. [PubMed: 19060566]
8. Eilken HM, Adams RH. Dynamics of endothelial cell behavior in sprouting angiogenesis. Current opinion in cell biology. 2010; 22:617–625. [PubMed: 20817428]
9. Huang Y, Hoffman C, Rajappa P, Kim JH, Hu W, et al. Oligodendrocyte progenitor cells promote neovascularization in glioma by disrupting the blood-brain barrier. Cancer research. 2014; 74:1011–1021. [PubMed: 24371228]
10. Aghi M, Cohen KS, Klein RJ, Scadden DT, Chiocca EA. Tumor stromal-derived factor-1 recruits vascular progenitors to mitotic neovasculature, where microenvironment influences their differentiated phenotypes. Cancer research. 2006; 66:9054–9064. [PubMed: 16982747]
11. Du R, Lu KV, Petritsch C, Liu P, Ganss R, et al. HIF1alpha induces the recruitment of bone marrow-derived vascular modulatory cells to regulate tumor angiogenesis and invasion. Cancer cell. 2008; 13:206–220. [PubMed: 18328425]
12. Achyut BR, Shankar A, Iskander AS, Ara R, Angara K, et al. Bone marrow derived myeloid cells orchestrate antiangiogenic resistance in glioblastoma through coordinated molecular networks. Cancer letters. 2015; 369:416–426. [PubMed: 26404753]
13. Arbab AS. Activation of alternative pathways of angiogenesis and involvement of stem cells following anti-angiogenesis treatment in glioma. Histology and histopathology. 2012; 27:549–557. [PubMed: 22419019]
14. Rivera LB, Meyronet D, Hervieu V, Frederick MJ, Bergsland E, et al. Intratumoral myeloid cells regulate responsiveness and resistance to antiangiogenic therapy. Cell reports. 2015; 11:577–591. [PubMed: 25892230]
15. Seto T, Kato T, Nishio M, Goto K, Atagi S, et al. Erlotinib alone or with bevacizumab as first-line therapy in patients with advanced non-squamous non-small-cell lung cancer harbouring EGFR

mutations (JO25567): an open-label, randomised, multicentre, phase 2 study. The Lancet. Oncology. 2014; 15:1236–1244. [PubMed: 25175099]

16. Thon N, Kreth S, Kreth FW. Personalized treatment strategies in glioblastoma: MGMT promoter methylation status. Onco Targets Ther. 2013; 6:1363–1372. [PubMed: 24109190]
17. Yuen DA, Stead BE, Zhang Y, White KE, Kabir MG, et al. eNOS deficiency predisposes podocytes to injury in diabetes. Journal of the American Society of Nephrology: JASN. 2012; 23:1810–1823. [PubMed: 22997257]
18. Jacobs VL, Valdes PA, Hickey WF, De Leo JA. Current review of in vivo GBM rodent models: emphasis on the CNS-1 tumour model. ASN neuro. 2011; 3:e00063. [PubMed: 21740400]
19. Achyut BR, Shankar A, Iskander AS, Ara R, Knight RA, et al. Chimeric Mouse Model to Track the Migration of Bone Marrow Derived Cells in Glioblastoma Following Anti-angiogenic Treatments. Cancer biology & therapy. 2016
20. Obacz J, Pastorekova S, Vojtesek B, Hrstka R. Cross-talk between HIF and p53 as mediators of molecular responses to physiological and genotoxic stresses. Molecular cancer. 2013; 12:93. [PubMed: 23945296]
21. Bhaskara VK, Sundaram C, Babu PP. pERK, pAkt and pBad: a possible role in cell proliferation and sustained cellular survival during tumorigenesis and tumor progression in ENU induced transplacental glioma rat model. Neurochemical research. 2006; 31:1163–1170. [PubMed: 16944316]
22. McAllister SD, Christian RT, Horowitz MP, Garcia A, Desprez PY. Cannabidiol as a novel inhibitor of Id-1 gene expression in aggressive breast cancer cells. Molecular cancer therapeutics. 2007; 6:2921–2927. [PubMed: 18025276]
23. Paulis YW, Huijbers EJ, van der Schaft DW, Soetekouw PM, Pauwels P, et al. CD44 enhances tumor aggressiveness by promoting tumor cell plasticity. Oncotarget. 2015
24. Miletic H, Niclou SP, Johansson M, Bjerkvig R. Anti-VEGF therapies for malignant glioma: treatment effects and escape mechanisms. Expert opinion on therapeutic targets. 2009; 13:455–468. [PubMed: 19335067]
25. Domingues I, Rino J, Demmers JA, de Lanerolle P, Santos SC. VEGFR2 translocates to the nucleus to regulate its own transcription. PloS one. 2011; 6:e25668. [PubMed: 21980525]
26. Fox SB, Turley H, Cheale M, Blazquez C, Roberts H, et al. Phosphorylated KDR is expressed in the neoplastic and stromal elements of human renal tumours and shuttles from cell membrane to nucleus. The Journal of pathology. 2004; 202:313–320. [PubMed: 14991896]
27. Francescone R, Scully S, Bentley B, Yan W, Taylor SL, et al. Glioblastoma-derived tumor cells induce vasculogenic mimicry through Flk-1 protein activation. J Biol Chem. 2012; 287:24821–24831. [PubMed: 22654102]
28. Mesti T, Savarin P, Triba MN, Le Moyec L, Ocvirk J, et al. Metabolic impact of anti-angiogenic agents on U87 glioma cells. PloS one. 2014; 9:e99198. [PubMed: 24922514]
29. Jiang F, Zhang X, Kalkanis SN, Zhang Z, Yang H, et al. Combination therapy with antiangiogenic treatment and photodynamic therapy for the nude mouse bearing U87 glioblastoma. Photochemistry and photobiology. 2008; 84:128–137. [PubMed: 18173712]
30. Candolfi M, Curtin JF, Nichols WS, Muhammad AG, King GD, et al. Intracranial glioblastoma models in preclinical neuro-oncology: neuropathological characterization and tumor progression. Journal of neuro-oncology. 2007; 85:133–148. [PubMed: 17874037]
31. de Vries NA, Beijnen JH, van Tellingen O. High-grade glioma mouse models and their applicability for preclinical testing. Cancer treatment reviews. 2009; 35:714–723. [PubMed: 19767151]
32. Aparicio S, Hidalgo M, Kung AL. Examining the utility of patient-derived xenograft mouse models, Nature reviews. Cancer. 2015; 15:311–316.

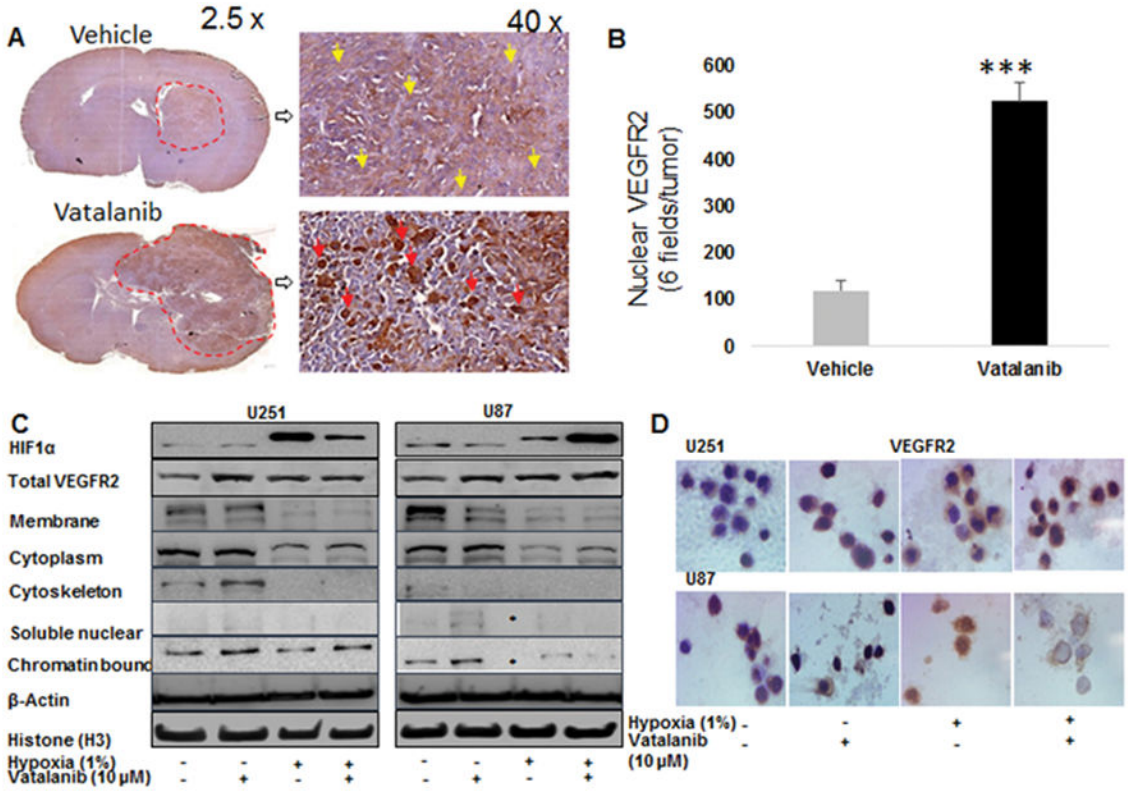

Figure 1. Anti-VEGFR2 induced nuclear translocation of VEGFR2 in GBM

(A) Immunohistochemical analysis on vehicle and vatalanib treated tumor tissues (n=3). Left panels showing tumor areas in whole brain (2.5 X). Middle panel showing VEGFR2 expression in enlarged (40 X) tumor sections. Vehicle treated tumors displayed mostly membrane bound VEGFR2 (yellow arrows). Vatalanib treated tumors displayed increased nuclear VEGFR2 (red arrows). **(B)** Quantitative data showing significant increased nuclear VEGFR2 in vatalanib treated tumors compared to vehicle. **(C)** Western blot data showing protein expression of HIF1α, total VEGFR2 and VEGFR2 expression in cellular compartments of U251 and U87 in response to vehicle and vatalanib (10μM) treatment under normoxic and hypoxic conditions. **(D)** Immunohistochemical analysis on cultured U251 and U87 tumor-cell smears showing nuclear expression of VEGFR2 along with vehicle vs. vatalanib treatment as well as normoxia vs. hypoxia. Shown is one of the two experiments performed. Quantitative data is expressed in mean ±SD and ***P<0.001.

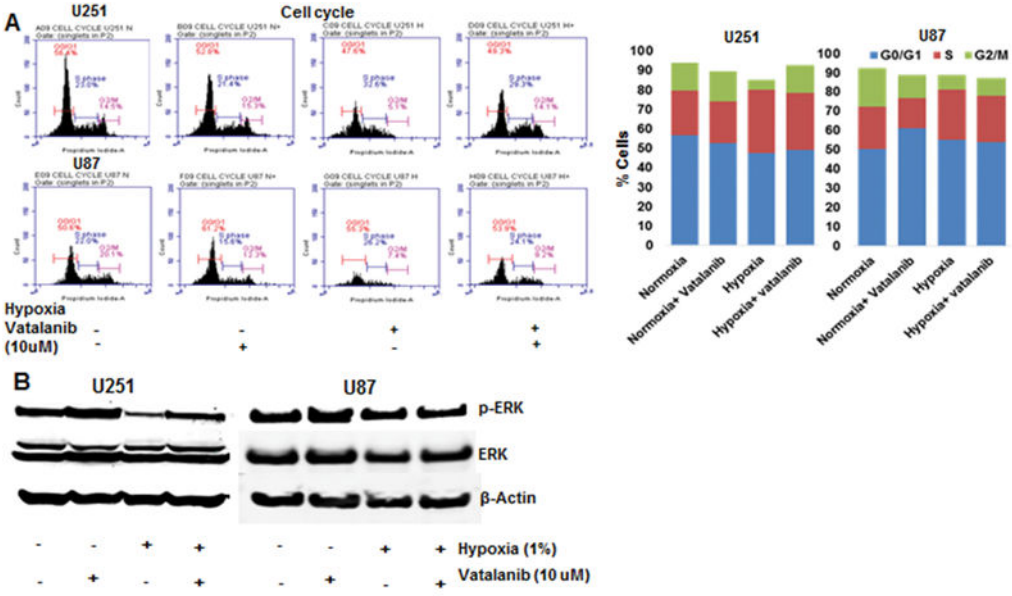

Figure 2. Vatalanib treatment induced cell cycle and proliferations of GBM cells

(A) Cell cycle analysis of U251 and U87 cells showing effect of vatalanib treatment on G0/G1, S and G2/M phases under normoxia and hypoxia. In U251 cells, vatalanib treatment showed modest effect on G0/G1, S and G2/M phases under normoxia compared to vehicle group. Vatalanib significantly increased G2/M phase under hypoxia condition compared to vehicle (5.1% vs 14.1%). In U87 cells, vatalanib treatment resulted into G0/G1 arrest under normoxia compared to vehicle (50.6% vs 61.2%). Vatalanib treatment showed modest effect on G0/G1, S and G2/M phases under hypoxia compared to vehicle. **(B)** Western blot showing vatalanib induced ERK expression in U251 and U87 cells under normoxia and hypoxia. In U251 cells, vatalanib treatment increased phospho-ERK expression both in normoxia and hypoxia. No change was seen in phospho-ERK expression in U87 cells. Shown is one of the two experiments performed.

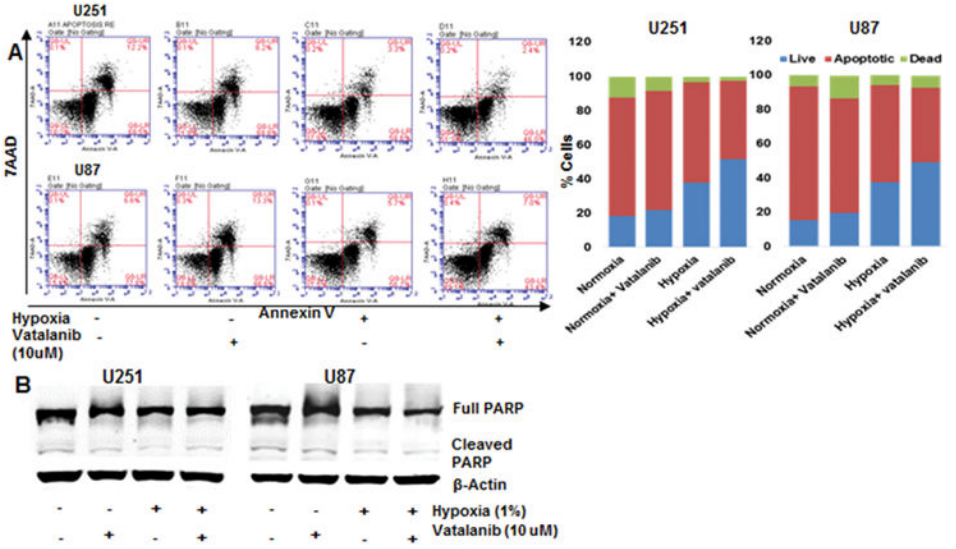

Figure 3. Vatalanib treatment decreased apoptosis of GBM cells

(A) Flow cytometry data showing annexin V staining on U251 and U87 cells. In U251 cells, normoxia group displayed increased viability (21.8% vs 18.2%), and decreased dead cells (8.2% vs 12.2%) with no change in apoptosis (69.8% vs 69.5%) with vatalanib compared to vehicle, respectively. Hypoxia resulted in increased viable cells (51.3% vs 37.9%), decreased dead cells (2.4% vs 3.3%) and decreased apoptotic cells (46% vs 58.6%) with vatalanib compared to vehicle, respectively (left and right panels). In U87 cells, vatalanib treatment under normoxia increased live cells (19.8% vs 15.4%), increased dead cells (13.3% vs 6.6%) and decreased apoptotic cells (66.6% vs 77.8%) compared to vehicle, respectively. Similarly, vatalanib under hypoxia increased U87 cell viability (49.1% vs 37.5%), decreased apoptotic cells (43.4% vs 56.7%) and increased dead cells (7% vs 5.7%), respectively (left and right panels). **(B)** Western blot data showing decreased cleaved PAPR expression in both U251 and U87 cells under hypoxia compared to normoxia. Shown is one of the two experiments performed.

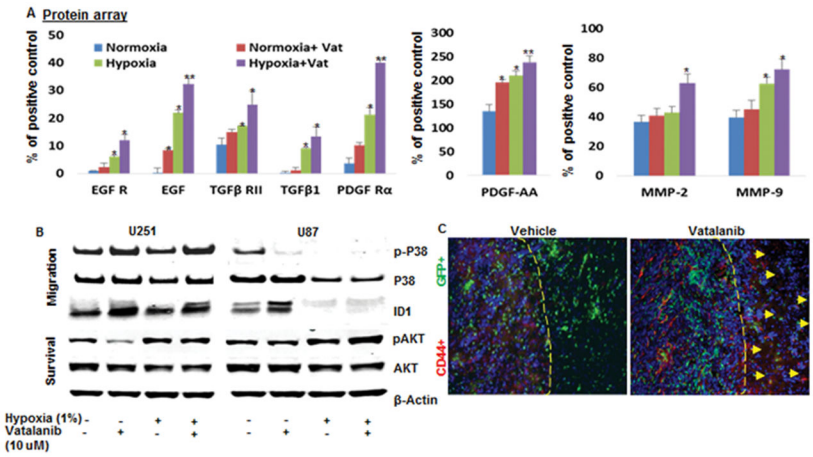

Figure 4. Vatalanib treatment induced invasion and migration of U251 cells

(A) Membrane protein array data showing significant overexpression of chemokines and their receptors (EGF-EGFR, TGFB1-TGFBR2, PDGFAA-PDGFRA, MMP2 and MMP9) in tumor conditioned medium following vatalanib treatment compared to vehicle, especially under hypoxia. **(B)** Western blot data showing increased phospho-P38 and ID1 protein expression in U251 cells both under normoxia and hypoxia, following vatalanib treatment compared to vehicle. In U87 cells, vatalanib decreased phospho-P38 expression under normoxia compared to vehicle group. 1D1 expression was increased after vatalanib treatment under normoxia compared to vehicle group. However, hypoxia significantly decreased ID1 expression and did not change with vatalanib. Overall, p-AKT was upregulated in hypoxia compared to normoxia in both U251 and U87. Interestingly, vatalanib decreased p-AKT compared to vehicle under normoxia in U251 cells. Vatalanib increased p-AKT compared to vehicle under hypoxia in U87 cells. **(C)** Vatalanib treated tumor showing increased CD44+ invasive tumor cells by immunofluorescence staining. Invasive front in vatalanib group was characterized by the CD44+ tumor cells, which were migrating away from the tumor periphery (yellow arrows). Shown is one of the two experiments performed. Quantitative data is expressed in mean ±SD. * P<0.05 and **P<0.01.